frontiers | Frontiers in Physiology

ORIGINAL RESEARCH
published: 29 August 2022
doi: 10.3389/fphys.2022.913443

A Comparison of MRI Quantitative Susceptibility Mapping and TRUST-Based Measures of Brain Venous Oxygen Saturation in Sickle Cell Anaemia

*Russell Murdoch[1†], Hanne Stotesbury[2†], Patrick W. Hales[2], Jamie M. Kawadler[2], Melanie Kölbel[2], Christopher A. Clark[2], Fenella J. Kirkham[2,3] and Karin Shmueli[1]**

[1]Department of Medical Physics and Biomedical Engineering, University College London, London, United Kingdom, [2]Developmental Neurosciences, UCL Great Ormond Street Institute of Child Health, London, United Kingdom, [3]Clinical and Experimental Sciences, University of Southampton, Southampton, United Kingdom

OPEN ACCESS

Edited by:
Ozlem Yalcin,
Koç University, Turkey

Reviewed by:
Banu Oflaz Sözmen,
Koç University, Turkey
Umut A. Gurkan,
Case Western Reserve University, United States

***Correspondence:**
Karin Shmueli
k.shmueli@ucl.ac.uk

[†]These authors have contributed equally to this work and share first authorship

Specialty section:
This article was submitted to Red Blood Cell Physiology, a section of the journal Frontiers in Physiology

Received: 05 April 2022
Accepted: 15 June 2022
Published: 29 August 2022

Citation:
Murdoch R, Stotesbury H, Hales PW, Kawadler JM, Kölbel M, Clark CA, Kirkham FJ and Shmueli K (2022) A Comparison of MRI Quantitative Susceptibility Mapping and TRUST-Based Measures of Brain Venous Oxygen Saturation in Sickle Cell Anaemia. Front. Physiol. 13:913443. doi: 10.3389/fphys.2022.913443

In recent years, interest has grown in the potential for magnetic resonance imaging (MRI) measures of venous oxygen saturation (Y_v) to improve neurological risk prediction. T_2-relaxation-under-spin-tagging (TRUST) is an MRI technique which has revealed changes in Y_v in patients with sickle cell anemia (SCA). However, prior studies comparing Y_v in patients with SCA relative to healthy controls have reported opposing results depending on whether the calibration model, developed to convert blood T_2 to Y_v, is based on healthy human hemoglobin (HbA), bovine hemoglobin (HbBV) or sickle hemoglobin (HbS). MRI Quantitative Susceptibility Mapping (QSM) is an alternative technique that may hold promise for estimating Y_v in SCA as blood magnetic susceptibility is linearly dependent upon Y_v, and no significant difference has been found between the magnetic susceptibility of HbA and HbS. Therefore, the aim of this study was to compare estimates of Y_v using QSM and TRUST with five published calibration models in healthy controls and patients with SCA. 17 patients with SCA and 13 healthy controls underwent MRI. Susceptibility maps were calculated from a multi-parametric mapping acquisition and Y_v was calculated from the mean susceptibility in a region of interest in the superior sagittal sinus. TRUST estimates of T_2, within a similar but much smaller region, were converted to Y_v using five different calibration models. Correlation and Bland-Altman analyses were performed to compare estimates of Y_v between TRUST and QSM methods. For each method, t-tests were also used to explore group-wise differences between patients with SCA and healthy controls. In healthy controls, significant correlations were observed between QSM and TRUST measures of Y_v, while in SCA, there were no such correlations. The magnitude and direction of group-wise differences in Y_v varied with method. The TRUST-HbBV and QSM methods suggested decreased Y_v in SCA relative to healthy controls, while the TRUST-HbS ($p < 0.01$) and TRUST-HbA models suggested increased Y_v in SCA as in previous studies. Further validation of all MRI measures of Y_v, relative to ground truth measures such as O^{15} PET and jugular vein catheterization, is required in SCA before QSM or TRUST methods can be considered for neurological risk prediction.

Keywords: sickle cell anaemia, T2-relaxation-under-spin-tagging, quantitative susceptibility mapping, venous oxygen saturation, validation, magnetic resonance imaging

1 INTRODUCTION

Sickle cell anemia (SCA) is an inherited blood disorder characterized by hemolytic anemia, vasculopathy, cognitive difficulties and high incidence of ischemic stroke, and silent cerebral infarction (Debaun and Kirkham 2016; Stotesbury et al., 2019). The mechanism for these complications in SCA are poorly understood and current methods of risk prediction in SCA are non-specific and have not been validated in adults (Stotesbury et.al., 2018; Stotesbury et al., 2021).

Interest has grown in the potential for magnetic resonance imaging (MRI) estimates of venous oxygen saturation (Y_v), and the closely related oxygen extraction fraction (OEF), to improve neurological risk prediction in SCA (Jordan and DeBaun 2018). Measuring Y_v *in-vivo* is challenging, and all oxygen-sensitive MRI techniques rely on models to convert the MRI measures into Y_v. Questions remain around the validity of these models, particularly in conditions such as SCA where alterations in blood rheology and oxygen-carrying capacity may challenge model assumptions.

In this study we aimed to compare measures of Y_v in SCA, and healthy controls (HC) subjects, derived from two MRI methods: T_2-relaxation-under-spin-tagging (TRUST) and the more recently developed quantitative susceptibility mapping (QSM).

TRUST is based on the principle that the transverse relaxation time of blood (T_{2b}) is dependent on its oxygen saturation (Lu et al., 2012) and has been widely used to estimate Y_v. TRUST applies similar principles to arterial spin labelling (ASL) to isolate the signal from venous blood, and uses T_2 preparation pulses to acquire signal at a series of effective echo times (eTE). The venous blood T_2 is then estimated from an exponential fit of the signal from venous blood (ΔS) as a function of eTE:

$$\Delta S = \Delta S_0 \cdot e^{eTE \cdot \left(\frac{1}{T_{1b}} - \frac{1}{T_{2b}} \right)} \quad (1)$$

Where ΔS_0 is the signal intensity difference at eTE = 0 and T_{1b} is the longitudinal relaxation time of venous blood.

Five calibration models have been previously developed to convert the venous blood T_2 measured using TRUST to Y_v: one based on bovine-hemoglobin (HbBV) (Lu et al., 2012; Jordan et al., 2016), one on hemoglobin-A (HbA) (Bush et al., 2017), and three derived from hemoglobin-S: HbS_{Bush} (Bush et al., 2018), HbS_{Li} (Li et al., 2020) and $HbS_{Li\text{-}Bush}$ (Bush et al., 2021). These models are described in detail in the **Supplementary materials**. Using TRUST, Y_v can appear either increased or decreased in SCA relative to healthy controls depending on the calibration model used (Lin et al., 2022). An overview of published studies applying TRUST in SCA subjects is shown in **Table 1**.

QSM is a more recent MRI technique that reconstructs the spatial distribution of magnetic susceptibility (χ) from gradient-echo (GRE) phase images (Shmueli 2020). QSM measures of Y_v are based on the observation that hemoglobin in its oxygenated form is weakly diamagnetic, while deoxygenated hemoglobin is

TABLE 1 | Overview of the previous literature investigating the effect of sickle cell anemia (SCA) on venous oxygen saturation (Y_v) and oxygen extraction fraction (OEF) relative to healthy controls (HC). Abbreviations: T2-relaxation-under-spin-tagging (TRUST), asymmetric spin echo (ASE), positron emission tomography (PET).

MRI TRUST Studies

Author	Year	Calibration model	Number of SCA subjects (age mean ± S.D., years)	Number of healthy control (HC) subjects (age mean ± S.D., years)	Results
Jordan et al. (2016)	2016	HbBV	27 (27.7 ± 5.0)	11 (26.9 ± 5.1)	Y_v decreased in SCA vs. HC (52.0 ± 7.5% vs. 63.2 ± 6.1%, $p < 0.05$)
Bush et al. (2018)	2017	HbS_{Bush}	33 (21.8 ± 9.0)	37 (27.2 ± 10.6)	Y_v increased in SCA vs. HC (73 ± 5% vs. 61 ± 6%, $p < 0.0001$)
Li et al. (2020)	2019	Subject Specific	11 (25 ± 7)	12 (35 ± 7)	No significant OEF differences between SCA and HC (37.5 ± 5% vs. 38.9 ± 5% $p = 0.31$)
Vu et al. (2021)	2021	$HbS_{Li\text{-}Bush}$	47 (21.7 ± 7.1)	44 (26.4 ± 10.6)	OEF significantly decreased in SCA vs. HC (27.4 ± 4.1% vs. 36.7 ± 6.0%, $p < 0.01$)

MRI QSM Studies

Author	Year	ROI	Number of SCA subjects	Number of Healthy Control (HC) subjects	Results
Shen et al. (2019)	2019	Straight Sinus	16 (24 ± 7)	11 (25 ± 9)	Y_v decreased in SCA vs. HC (69.3% vs. 73.9%, $p < 0.05$)
Murdoch et al. (2021)	2021	Superior Sagittal Sinus	88 (18.4 ± 10.0)	30 (18.0 ± 9.6)	Y_v decreased in SCA vs. HC (72.3 vs. 74.5, $p < 0.005$)

MRI and PET Whole Brain Studies

Author	Year	Method	Number of SCA subjects	Number of Healthy Control (HC) subjects	Results
Fields et al. (2018)	2017	ASE	36 (10.0)	20 (11.0)	Whole-brain OEF increased in SCA (42.7 vs. 28.8 $p < 0.001$)
Herold et al. (1986)	1986	O^{15} PET	6 (27.5 ± 8.7)	14 (34.3 ± 7.0)	No significant OEF differences (42 ± 4% vs. 44 ± 7%)

strongly paramagnetic. Therefore, the measured χ of venous blood relative to the surrounding tissue ($\Delta\chi_{vein-water}$, assuming that surrounding tissue has the same χ as water), should be directly proportional to the concentration of deoxygenated hemoglobin (Jain et al., 2012). $\Delta\chi_{vein-water}$ and Y_v are linearly related by the following expression (Weisskoff and Kiihne 1992):

$$Y_v = 1 - \frac{\Delta\chi_{vein-water} - \Delta\chi_{oxy-water} \cdot Hct}{\Delta\chi_{do} \cdot Hct} \quad (2)$$

Where hematocrit (Hct) is the percentage of erythrocytes in blood, $\Delta\chi_{do}$ is the χ shift between fully oxygenated and de-oxygenated erythrocytes [$0.27 \times 4\pi$ ppm (SI)] and $\Delta\chi_{oxy-water}$ is the χ shift between oxygenated erythrocytes and water [$-0.03 \times 4\pi$ ppm (SI)] (Weisskoff and Kiihne 1992).

QSM has been shown to be sensitive to changes in Y_v/OEF in conditions which affect cerebral oxygen metabolism and/or blood flow. Oxygen extraction fraction is defined as the arteriovenous difference in oxygen saturation, and increased OEF corresponds to decreased Y_v, for a given arterial oxygen saturation. QSM was sensitive to changes in hemispheric venous oxygen saturation in patients with acute stroke: increased QSM-based OEF was observed in cerebral veins in the affected hemisphere relative to the contralateral hemisphere (29.3 ± 3.4% versus 25.5 ± 3.1% $p < 0.032$) (Fan et al., 2020). QSM has also been applied in patients with arteriovenous malformations (AVMs), showing that veins draining AVMs had significantly higher Y_v compared to healthy veins as a result of arteriovenous shunting (Biondetti et al., 2019).

Previous work in a pilot study of 6 SCA patients and 6 healthy controls has demonstrated no significant χ difference between deoxyhemoglobin in sickle and normal erythrocytes, suggesting that QSM is valid in both SCA and healthy controls (HC) (Eldeniz et al., 2021). To date, only two studies of Y_v in SCA have been carried out using QSM, with both studies reporting decreased Y_v in SCA relative to HC (Shen et al., 2019; Murdoch et al., 2021).

TRUST is a global measure of Y_v, derived from T_2 values fitted within a small region of interest (ROI) in the superior sagittal sinus (SSS) within a single slice. QSM can also be used to derive a similar global measure of Y_v by estimating the mean magnetic susceptibility within a ROI in the SSS. In QSM, the ROI can be a three-dimensional volume spanning several slices and including many more voxels than the region used in TRUST.

Aiming to improve our understanding of Y_v estimation in SCA, we compared measures of global Y_v derived from QSM and TRUST using each of the five calibration models.

2 MATERIALS AND METHODS

2.1 Patients

Patients with sickle cell anemia (SCA; hemoglobin-SS) and age matched healthy controls were recruited to two concurrent studies with overlapping MRI protocols between 2016 and 2019: the Sleep Asthma Cohort follow-up (SAC) (Rosen et al., 2014) and the Prevention of Morbidity in Sickle Cell Anemia baseline investigation (POMS) (Howard et al., 2018). Inclusion and exclusion criteria have been described elsewhere (Stotesbury et al., 2022). In 2018, the TRUST sequence was added to both MRI protocols as an optional sequence for participants who tolerated the core protocol. Participants from both studies with TRUST data were eligible for inclusion.

Fetal hemoglobin (HbF) concentration, absolute reticulocyte count (ARC) and lactate dehydrogenase (LDH) were not collected as part of this study. Steady state HbF concentration, ARC and LDH were available in participants recruited from the UK National Health Service (NHS) who consented for collection of this information for research purposes and not available in the patients recruited from the community (**Table 2**).

Ethical approval was granted by West London NHS (05/Q0408/42, 11/EM/0084, 15/LO/0347), Yorkshire NHS (15/YH/0213), and University College London (14475/001) ethics committees. Full informed consent and assent according to the Declaration of Helsinki were obtained from participants and, for children, from their parent/guardian.

2.2 MRI Acquisition

All participants were imaged on a 3T Siemens (Erlangen, Germany) Magnetom Prisma MRI System using a 64-channel head coil. The MRI protocol included a TRUST sequence with repetition time (TR) = 3000 ms, inversion time (TI) = 1020 ms, voxel size = $3.44 \times 3.44 \times 5\ mm^3$, matrix size = $64 \times 64 \times 1$, effective echo time (eTE) = 0, 40, 80, 160 ms, label slab = 100 mm and 3 averages. This was followed by a multi-parametric mapping (MPM) acquisition comprised of three fast low angle shot (FLASH) GRE sequences with respective magnetization transfer (MT), proton density (PD) and T_1 weighting. The PD-weighted sequence parameters were: TR = 24.5 ms, TE_1 = 2.34 ms, ΔTE = 2.34 ms, echoes = 8, flip angle = 6°, voxel size = $1\ mm^3$ isotropic. T_1-weighting was introduced by increasing the flip angle to 20° with all other parameters kept the same. MT-weighting was introduced by applying off-resonance saturation pulses prior to excitation with the number of echoes reduced to 6 to maintain consistent TR.

During the MRI examination, peripheral oxygen saturation (SpO_2) was measured using a pulse oximeter. Blood T1 was estimated from blood hematocrit and measured SpO_2 (Hales et al., 2016). In one SCA subject, pulse oximetry measures of SpO_2 were not available and the mean SpO_2 across SCA patients (97.47%) was used.

2.3 MRI Processing

2.3.1 TRUST Processing

For each eTE, difference images were calculated between the TRUST label and control images. An initial square ROI was manually drawn covering the superior sagittal sinus (SSS). The SSS ROI was defined by selecting the four voxels with the largest signal intensity in the difference image with the shortest eTE (eTE = 0 ms). Signal intensities in the difference images were averaged over all four voxels for each eTE and estimates of the venous T_2 (T_{2b}) were estimated from a fit of these intensities as a function of eTE (**Eq. 1**).

TABLE 2 | Overview of the sickle cell anemia (SCA) and healthy control (HC) subjects included in this study.

	SCA	HC
N	17	13
Age (Mean ± SD) (years)	20.1 ± 4.7	21.2 ± 3.9
Male/Female	9/8	4/9
SpO_2 (measured/estimated)	16/1	13/0
SpO_2 (Mean ± SD) (%)	97.5 ± 2.4	99.4 ± 0.8
Hematocrit (measured/estimated)	12/5	0/13
Hematocrit (Mean ± SD) (%)	26.3 ± 4.1	41.4 ± 3.3
Hemoglobin (Mean ± SD) (g/dl)	9.02 ± 1.47	NA
Hydroxyurea Treatment (Yes)	6 (35%)	NA
Transfusion Last 6 Months (Yes)	7 (41%)	NA
Chronic Transfusions (Yes)	3 (18%)	NA
Silent Cerebral Infarcts (Yes)	8 (47%)	2 (15%)
Previous Acute Chest Crisis (Yes) (n = 15)	9/15 (60%)	NA
Fetal Hemoglobin (Mean ± SD) (%) (n = 13)	8.75 ± 7.36	NA
Absolute Reticulocyte Count (ARC) (Mean ± SD) (cells/μl) (n = 8)	287 ± 105	NA
Lactate dehydrogenase (LDH) (Mean ± SD) (IU/L) (n = 15)	679 ± 354	NA

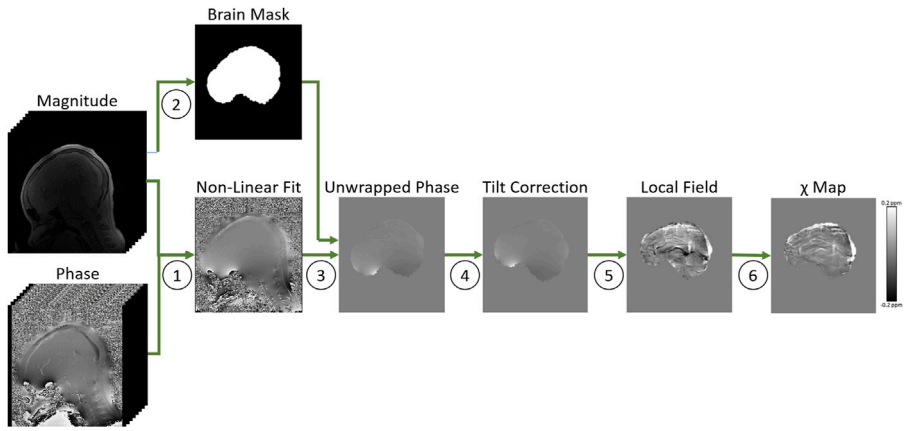

FIGURE 1 | Overview of the quantitative susceptibility mapping processing pipeline in a representative healthy control, applied to the MPM T1-weighted FLASH sequence. 1. Total field maps were estimated from a non-linear fit of the complex multi-echo images (Liu et al., 2013). 2. Brain masks were estimated using FSL brain extraction tool (Smith 2002). 3. Residual wraps in the field map were removed using SEGUE phase unwrapping (Karsa and Shmueli 2018). 4. Images were realigned with the B_0 direction (Kiersnowski et al., 2021). 5. Background field removal was performed using projection onto dipole fields (Liu et al., 2011) 6. Susceptibility maps were calculated using an iterative Tikhonov method (Karsa et al. 2020).

Venous oxygen saturation (Y_v) was estimated from T_{2b} using previously derived calibration models based on bovine (HbBV) and healthy (HbA) hemoglobin, as well as three models based on sickle hemoglobin; the Bush (HbS_{Bush}), Li (HbS_{Li}) and combined Li-Bush ($HbS_{Li\text{-}Bush}$) models. Full details on each model are provided in the **Supplementary materials**.

For the 12 SCA subjects with blood samples taken, measures of hematocrit from the blood drawn closest to the MRI examination were selected. In the remaining 5 SCA subjects, hematocrit was estimated as the mean hematocrit of this cohort (26.3%).

Study ethics did not cover taking blood samples from healthy control subjects and hematocrit had to be estimated. Not all controls in this study were race-matched to the SCA participants and hematocrit estimates in white and black controls were derived from two different sources. In the white control subjects (all aged 20–30) hematocrit was estimated as 0.47 in males and 0.42 in females (Kratz et al., 2004). In the black control subjects hematocrit was estimated from a study which investigated the effect of age and sex upon blood hematcrit values in healthy black Americans (Castro et al., 1987); estimated hematocrit values ranged from 0.35 to 0.42 depending upon patient demographic.

2.3.2 QSM Processing

Maps of magnetic susceptibility (χ) were calculated from each of the three MPM FLASH acquisitions in their own native space via the following pipeline: total field maps were estimated from a non-linear fit of the complex multi-echo images (Liu et al., 2013), residual wraps in the field map were removed using SEGUE phase unwrapping (Karsa and Shmueli 2018), brain masks were

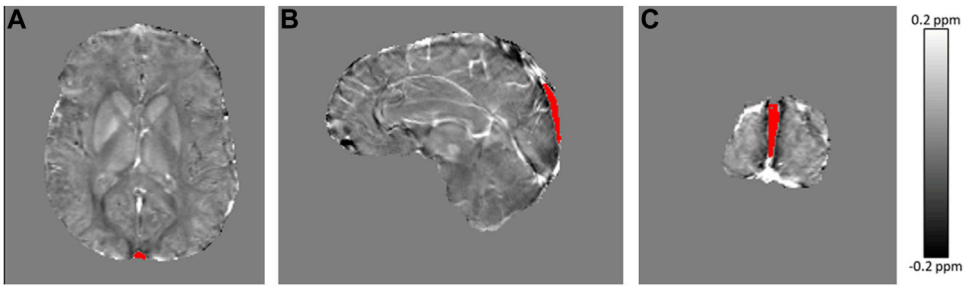

FIGURE 2 | Axial **(A)**, sagittal **(B)** and coronal **(C)** view of the average susceptibility map calculated across MPM acquisitions in a representative sickle cell anemia subject, with the segmented region of interest in the superior sagittal sinus overlaid in red.

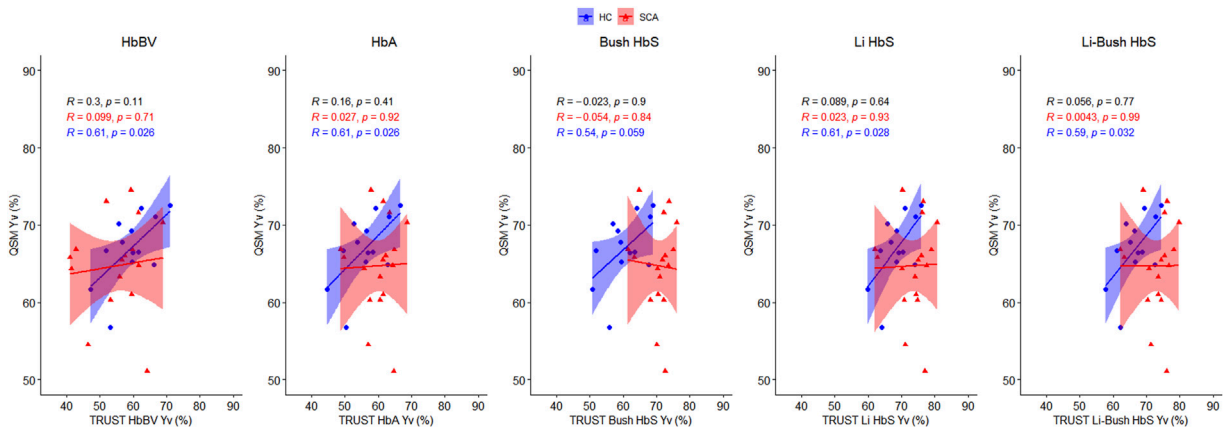

FIGURE 3 | Correlation between QSM and TRUST-based measures of venous oxygen saturation (Y_v) in sickle cell anemia (red) and healthy control subjects (blue). Pearson's correlation coefficients (r), and the corresponding *p* values, are shown for the combined cohort (black), and for the SCA (red) and healthy control (blue) groups. Shaded areas indicate the 95% confidence intervals of the linear regression.

estimated using FSL brain extraction tool (Smith 2002), to account for oblique acquisition images were realigned with the B_0 direction (Kiersnowski et al., 2021) prior to background field removal via projection onto dipole fields (Liu et al., 2011) and susceptibility maps were calculated using the iterative Tikhonov method (Karsa et al., 2020) (**Figure 1**). To account for head movement between acquisitions, the PD- and MT-weighted images were rigidly transformed into the T_1-w native space using NiftyReg (Modat et al., 2014). The average χ over the three MPM sequences was calculated to reduce noise (Murdoch et al., 2020). The mean χ was calculated in a ROI segmented in the SSS using a semi-automated approach in ITK-SNAP (Yushkevich et al., 2006) (**Figure 2**). This mean χ was then used to estimate Y_v *via* **Eq. 2**.

2.4 Statistical Analysis

Agreement between QSM and TRUST measures of Y_v was assessed using correlation and Bland-Altman analyses. Correlations were examined in the SCA and healthy control cohorts, in addition to the combined group. Bland-Altman analysis was carried out separately for the SCA and healthy controls groups. For each measure of Y_v, group-wise differences between SCA and HC cohorts were also explored using Student's t-tests.

3 RESULTS

Demographic, laboratory and clinical data are presented in **Table 2**. Steady state HbF concentrations were available in 13/17 participants with SCA, steady state absolute reticulocyte count (ARC) in 8/17 and lactate dehydrogenase (LDH) levels in 15/17 (**Table 2**). Compared with our cohort study (Stotesbury et al., 2022), the proportion of patients with SCA and SCI and the rates of hydroxyurea and blood transfusion treatment were similar.

Correlations between the QSM and TRUST-based measures of Y_v in patients with SCA and healthy controls are shown in **Figure 3**. In healthy controls, significant correlations were observed between QSM measures of Y_v and each of the TRUST-based measures, except for measures based on the Bush HbS calibration (p = 0.059). In patients with SCA, no such correlations were observed (**Figure 1**). The strongest

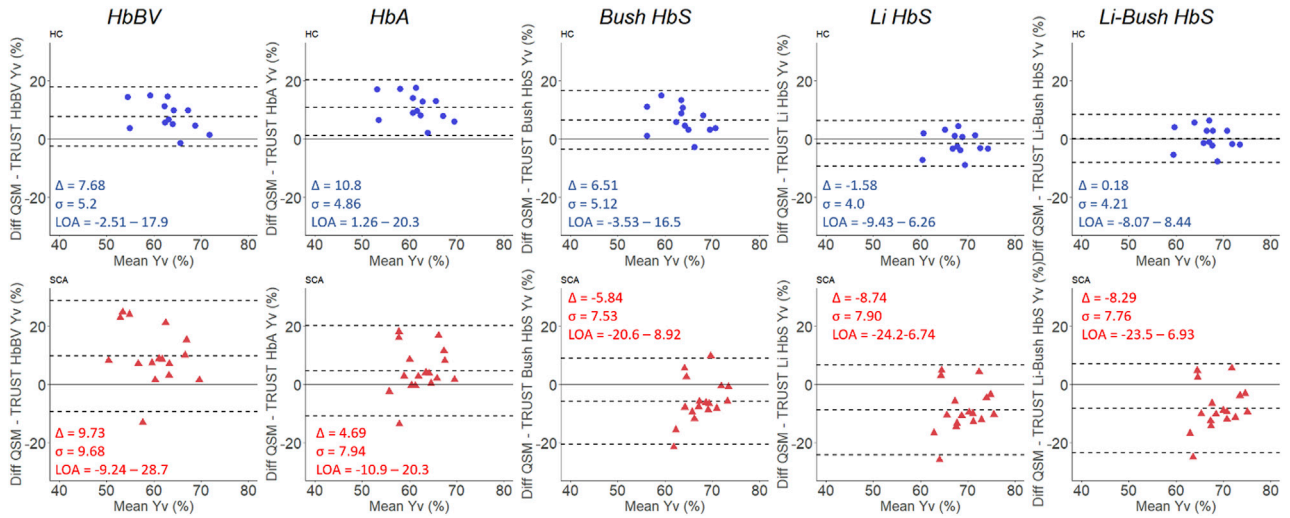

FIGURE 4 | Bland-Altman plots comparing QSM and TRUST-based measures of venous oxygen saturation (Y_v) in healthy control (blue: top) and sickle cell anemia (red: bottom) subjects. The mean bias (Δ) standard deviation of the bias (σ) and the limits of agreement (LOA) are shown for each plot.

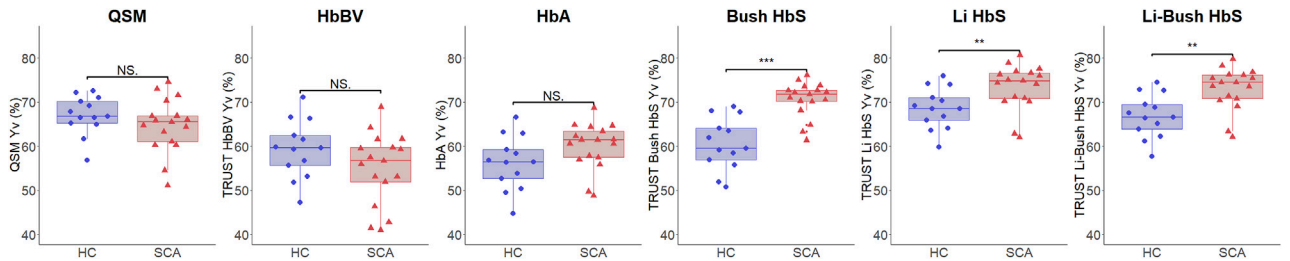

FIGURE 5 | Group wise comparison of mean venous oxygen saturation (Y_v, %, y-axis) measured in the superior sagittal sinus in sickle cell anemia (SCA) and healthy control (HC) subjects. One graph is shown for QSM of Y_v, and TRUST-based Y_v measures with five different calibration models. Mean differences between groups were examined by t-test: NS: no significant difference, $^{**}p < 0.01$, $^{***}p < 0.005$.

correlations in healthy controls were observed between QSM measures of Y_v and TRUST measures based on the HbBV (R = 0.61, $p = 0.026$) and HbA (R = 0.61, $p = 0.026$) calibration models. For the HbS calibration models in healthy controls, weaker correlations with QSM-based estimates of Y_v were observed. No correlations were observed between QSM- and TRUST-based measures of Y_v, in either the SCA or the combined group, for any of the TRUST calibration models.

The Bland-Altman analyses (**Figure 4**) showed wide variation in agreement between the QSM and TRUST-based measures of Y_v, with agreement heavily dependent upon the calibration model used, particularly in patients with SCA. In healthy controls, QSM Y_v estimates were higher relative to TRUST for most of the calibration models, with mean biases (Δ) of 7.6/10.8/6.5% observed for the HbBV/HbA/HbS_{Bush} models respectively. Smaller biases of −1.6% and 0.2% were found for the HbS_{Li} and $HbS_{Li\text{-}Bush}$ models respectively. In the SCA subjects, the direction of the mean bias varied with the calibration model. QSM Y_v estimates were higher relative to the HbBV and HbA calibration models (Δ = 9.7% and 4.7%) and lower relative to the three HbS models (Δ = −5.8/−8.7/−8.3%).

The significance and direction of group-wise differences in Y_v between patients with SCA and healthy controls depended on the T_2 calibration model used (**Figure 5**). Although not statistically significant, both the QSM (64.7% vs. 67.0%, $p = 0.23$) and the HbBV TRUST (55.0% vs. 59.4%, $p = 0.12$) models suggested numerically decreased Y_v in patients with SCA relative to healthy controls. The HbA model (60.0% vs. 56.2% $p = 0.09$), and the three HbS calibration models (HbS_{Bush}/HbS_{Li}/$HbS_{Li\text{-}Bush}$: 70.5% vs. 60.5%, $p < 0.001$/73.5% vs. 68.6%, $p = 0.011$/73.0% vs. 66.9%, $p = 0.002$) indicated significantly increased Y_v in patients with SCA relative to healthy controls.

4 DISCUSSION

QSM and TRUST based measures of Y_v were moderately correlated in healthy controls; however poor agreement

between methods was observed in patients with sickle cell anemia. Bland-Altman analyses showed the direction of biases between the QSM and TRUST-based measures of Y_v, were dependent upon the TRUST calibration model. Group-wise Y_v differences between SCA patients and healthy controls were further dependent upon the method used to measure Y_v and were in agreement with previously reported literature.

4.1 Agreement Between QSM and TRUST-Based Y_v

This study demonstrates poor agreement between measures of Y_v in the superior sagittal sinus derived from QSM and TRUST in patients with SCA. In patients with SCA, no significant correlations were observed between the QSM and TRUST measures, for any calibration model relating Y_v to the measured T_2 of venous blood. If both TRUST and QSM were accurately estimating Y_v, we would expect strong correlations between the two measures.

The Bland-Altman analysis shows that QSM tended to estimate higher Y_v in the superior sagittal sinus relative to TRUST in the healthy control subjects for the majority of calibration models. The χ of venous blood is determined by the concentration of paramagnetic deoxygenated hemoglobin. Therefore, a higher estimation of Y_v corresponds to a lower estimation of the χ in the superior sagittal sinus. This lower estimation may have been caused by inaccuracies in QSM in the SSS due to its location at the periphery of the brain mask. Any field perturbations outside of the brain, caused by the deoxygenated hemoglobin in the SSS, cannot be sampled, which will reduce the accuracy of χ and Y_v estimates in the vein. One of two published QSM studies of Y_v in SCA (Shen et al., 2019) considered χ values in the straight sinus and reported a mean Y_v of 69.3% vs. 73.9% in SCA vs. HC compared to 64.7% vs. 67.0% in the SSS in our study. Despite the straight sinus being far away from the edge of the brain mask, the estimates of Y_v in the straight sinus were even higher than in the SSS in our study. This may have been caused by partial volume effects in this venous structure, which is smaller than the SSS and more challenging to accurately segment, or could have been due to the use of L1 regularization in the χ map calculation which is known to underestimate venous χ (Berg et al., 2021). The choice of susceptibility calculation method has been shown to have a significant effect on estimates of Y_v, with Tikhonov-based regularization, as used in this study, shown to be the most accurate method for venous susceptibility measurement in a recent study (Berg et al., 2021).

In the SCA subjects, the direction of the bias between QSM and TRUST methods was dependent upon the calibration model employed. QSM Y_v measures were increased relative to the HbBV and HbA models and reduced relative to the three HbS models. Examining the Bland-Altman analysis, only the limits of agreement from the QSM-TRUST HbA comparison in healthy controls excluded zero and demonstrated a systematic bias.

4.2 Y_v in SCA vs. Healthy Controls

The results of the group-wise comparisons of Y_v in patients with SCA versus healthy controls largely agree with the results of previous studies investigating the effect of SCA on Y_v, and a recent comparison of the models in a pediatric population (Lin et al., 2022). An overview of these previous studies investigating Y_v in SCA is shown in **Table 1**, with results visualized in **Figure 6**. In the present study, the QSM results suggested numerically decreased Y_v in SCA relative to healthy controls. These results are in agreement with two prior studies using QSM to estimate Y_v in SCA (Shen et al., 2019; Murdoch et al., 2021). TRUST with the HbBV calibration model similarly suggested numerically decreased Y_v in SCA versus healthy controls; in agreement with the prior TRUST study in SCA that employed this model (Jordan et al., 2016). A decrease in Y_v in patients with SCA relative to healthy controls was also reported in a whole brain study that applied an asymmetric spin-echo based MRI-method and found that whole brain OEF was increased in SCA relative to HC (42.7% vs. 28.8%) (Fields et al., 2018), which is equivalent to a decrease in Y_v in SCA. However, in the present study, neither the QSM or TRUST HbBV Y_v differences between patients with SCA and HC reached significance.

Conversely, TRUST with each of the HbS calibration models found Y_v to be significantly increased in patients with SCA relative to healthy controls. TRUST with the HbA model also suggested elevated Y_v in SCA but the difference did not reach significance. Our TRUST results using HbS calibration models are in agreement with the results of two TRUST studies in larger cohorts which applied the HbS_{Bush} and $HbS_{Li\text{-}Bush}$ calibration models respectively (Bush et al., 2018; Vu et al., 2021).

Oxygen metabolism in the brain is measured by the cerebral metabolic rate of oxygen ($CMRO_2$) which is given by

$$CMRO_2 = C_a \cdot OEF \cdot CBF \tag{3}$$

where C_a is the arterial oxygen content, the product of C_a and OEF is the arteriovenous difference in oxygen saturation, and CBF is the cerebral blood flow.

$CMRO_2$ must be maintained to meet the oxygen demands of the brain, and ischemic stroke occurs when insufficient oxygen is delivered to tissue. In SCA, C_a is diminished as result of hemolysis and the corresponding reduction in blood hematocrit. It has been shown that CBF increases in SCA to compensate for the reduced arterial content (Bush et al., 2016). It has been hypothesized that OEF might increase in SCA to overcome the reduced C_a caused by anemia and in some cases oxygen desaturation. The studies reporting a decreased OEF in SCA have attributed this change to arteriovenous shunting (Stotesbury et al., 2019). If OEF is decreased in SCA, corresponding to increased Y_v, any CBF increase must be sufficiently large to compensate for the decreased C_a and OEF and ensure sufficient oxygen is supplied to tissue. There is little evidence that CMRO2 is diminished in SCA as the only published O^{15} PET study comparing patients with SCA and healthy controls reported no significant $CMRO_2$ differences between the two cohorts (Herold et al., 1986).

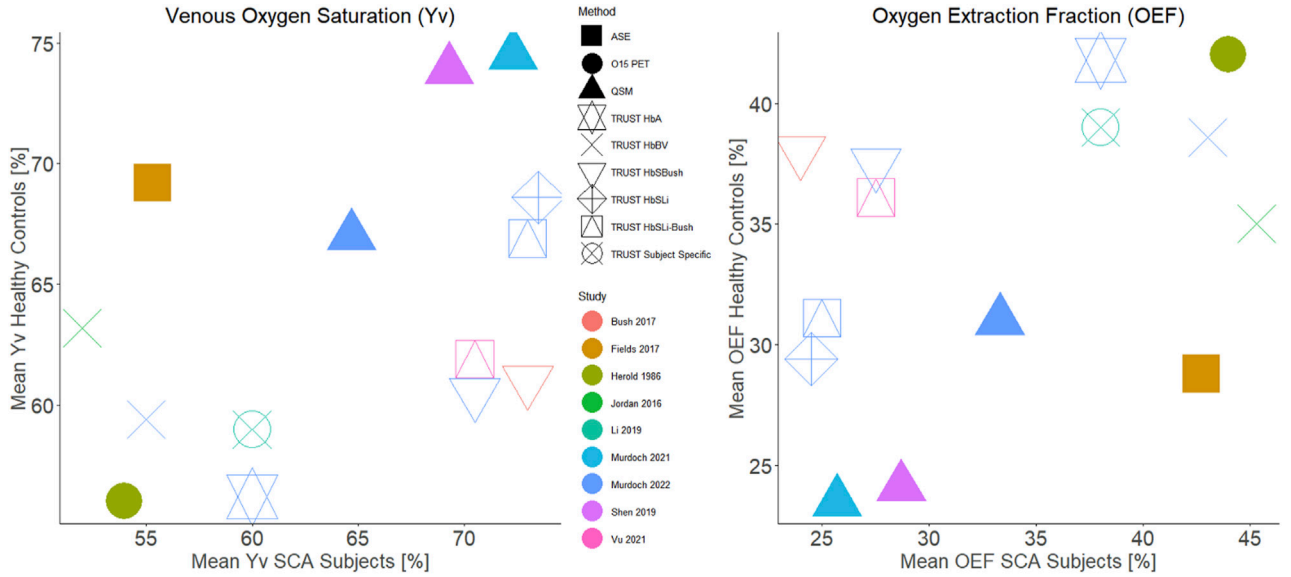

FIGURE 6 | Comparison of group mean venous oxygen saturation **(left)** and oxygen extraction fraction **(right)** in sickle cell anemia and healthy controls cohorts reported in previous literature. The points are colour coded by study and have symbols corresponding to the measurement technique used. For studies which did not report both the oxygen extraction fraction and venous oxygen saturation, the missing values were calculated assuming an arterial oxygenation of 98%.

4.3 Validation of QSM and TRUST-Based Measures of Y_v

One limitation of our study is the lack of a gold-standard measure of Y_v, such as O^{15} PET or jugular vein catheterization, which precluded investigation of the relative accuracy of the QSM and TRUST methods with each of the calibration models, beyond comparison with previously reported values. The Herold et al. PET study found no significant OEF differences between SCA and healthy control groups (SCA: 44% vs. HC: 42%). Y_v measures from QSM and TRUST with each of the calibration models can be compared with O^{15} PET estimates of Y_v: OEF = 44% corresponds to Y_v = 54% for an assumed arterial oxygen saturation of 98%. In patients with SCA, the TRUST HbBV model provided the closest estimate to the reported PET value (55%) whilst the TRUST method using the Li HbS and Li-Bush HbS calibration models (Y_v = 73.5% and 73.0% respectively), had the largest difference and may plausibly overestimate Y_v in SCA (**Figure 6**). However, it must be noted that the Herold study was conducted in a small population, and additional confounding factors will affect Y_v measures, including patient treatment.

In SCA patients, neither TRUST nor QSM measures of Y_v have been validated against gold standard measures. In other populations, QSM-derived OEF has also been compared with gold-standard O^{15} PET measures of OEF. Kudo et al. compared whole brain OEF measured from QSM using an approach reported by Zaitsu et al. (2011) to the gold-standard O^{15} PET OEF Kudo et al. (2016). The whole brain OEF maps were estimated from QSM by thresholding the χ maps to extract a venous map, and Y_v was estimated within each vein from the difference between the mean χ in each venous voxel relative to the χ in the surrounding brain parenchyma. OEF was estimated from 1-Y_v and a sliding window method was applied within slices to generate venous OEF maps. Significant correlations were observed between QSM and PET OEF measures at a hemispheric level, and QSM-OEF was sensitive to increased hemispherical OEF in patients with chronic unilateral internal carotid or middle cerebral artery stenosis or occlusion.

4.4 Limitations of QSM and TRUST Estimation of Y_v in SCA

TRUST can currently only provide an estimate of global Y_v from just a few voxels whereas QSM can provide Y_v estimates throughout the venous vasculature. The relatively large dimensions of the TRUST voxels (~59 mm^3) relative to the QSM voxels (1 mm^3) limited the number of voxels used to estimate venous T_2 to 4, whilst the mean number of voxels used to estimate the mean χ was orders of magnitude greater (mean ± standard deviation = 1225 ± 793). QSM can be affected by partial volume effects, with the inclusion of non-blood tissue within the ROI likely to result in reduction of the apparent venous χ and overestimation of Y_v. However, the large size of the superior sagittal sinus compared to the QSM voxel size minimizes the risk of partial volume effects (McFadden et al., 2021). In contrast to QSM, the image subtraction performed in TRUST removes signal from static tissue, ensuring that only venous blood contributes to the measured signal.

The TRUST signal model outlined in **Eq. 1** shows that the TRUST signal differences are dependent upon both T_1 and T_2 relaxation times. The majority of previous studies have estimated the venous blood T_1 from measured hematocrit levels but T_1 is also dependent on the venous blood oxygenation (Hales et al.,

2016). In our study, venous blood T_1 was estimated using a model developed by Hales et al. (Hales et al., 2016) based on the estimated hematocrit and arterial oxygen saturation measured using pulse oximetry. Pulse oximetry provides an estimate of arterial oxygenation but it is unlikely to accurately represent the venous oxygen saturation, adding another potential confound into TRUST oxygenation measurements.

An alternative method for estimating blood T_1 is to use MRI multi-parametric mapping (MPM), a quantitative imaging method which provides high resolution maps of parameters including T_1 (Lutti et al., 2013). This method is likely more accurate than using the model based on hematocrit and peripheral arterial oxygenation. Here, we used MPM T_1 maps to calculate the mean T_1 within the SSS ROI (used to estimate venous χ), to provide an alternative measure of blood T_1. Despite differences between the MPM-measured and Hales model-estimated blood T_1 values, these had a negligible effect on the T_{2b} values estimated by fitting **Eq. 1** (**Supplementary Materials**). This suggests that using estimated blood T_1 values was not a substantial source of error/inaccuracy in the TRUST results in this study.

The study by Li et al. suggested that individual TRUST T2 calibration models may be required for each SCA patient as blood T2 is dependent upon factors beyond Hct and Yv (Li et al., 2020). Red blood cell shape and the concentration of fetal hemoglobin in the blood were suggested as potential confounds to the T2 calibration model. Fetal haemoglobin (HbF) differs from adult haemoglobin (HbA) in the globular protein subunits: HbA is comprised of two alpha and two beta subunits, whilst HbF consists of two alpha and two gamma subunits. As the magnetic susceptibility of hemoglobin is determined by oxygenation dependent differences in the electron configuration of the heme iron centres, it is probable that the magnetic susceptibility of deoxygenated HbA and HbF are comparable, but this will require validation.

Hydroxyurea and blood transfusions are known to affect the relative concentrations of HbF and HbA and, given that HbF has a higher oxygen affinity than HbA, these therapies may, therefore, influence venous oxygen saturation. For the 13 patients with sickle cell anemia where steady state fetal hemoglobin levels were available, only 1 patient receiving hydroxyurea had unusually elevated HbF levels (>20%). Therefore, elevated HbF levels in the SCA cohort are unlikely to have had a confounding effect on the groupwise comparison results shown in **Figure 5**.

Future validation of QSM measures of Yv in patients with SCA would be strengthened by measuring the hemoglobin composition to investigate any potential confounding effects of the proportion of HbF/HbA/HbS.

Blood rheology has been shown to be modified in patients with sickle cell anemia (Connes et al., 2016). QSM and TRUST models are dependent upon blood hematocrit levels, a key determinant of blood viscosity. However, the possible effects of blood rheology on venous T2, flow and oxygenation in SCA or the potential effects of increased fibrinogen levels on blood susceptibility have not been investigated and could be explored in future work.

Accurate MRI measures of venous oxygen saturation in patients with sickle cell anemia would provide a useful biomarker when evaluating the efficacy of novel treatments. Of particular interest would be hemoglobin oxygen modifying therapies, for example Voxelotor (Oxbryta), which aims to reduce sickling by stabilizing HbS in an oxygenated state (Herity et al., 2021). It would be expected that prevention of HbS sickling would increase arterial oxygen capacity and, therefore, venous oxygen saturation, which could be quantified using the MRI measures compared in this study.

This study is limited by the relatively low numbers of patients with SCA and healthy controls, as well as by the use of estimated hematocrit values for 5/17 SCA subjects and all the healthy control subjects. QSM measures of Y_v were restricted to the SSS for the purpose of comparison with the TRUST results, which are limited to the SSS due to the low resolution, coverage and SNR of the TRUST MRI acquisition. QSM can provide local measures of Y_v in any venous structures which can be segmented (McFadden et al., 2021). We would expect localized changes in Y_v in SCA, as evidenced by the high incidence of ischemic stroke in the internal carotid and middle cerebral artery territories (Adams 1995; Pavlakis and Levinson 2009). Any localized changes in Y_v in SCA may only have a small effect in the SSS as many veins drain into the SSS, and future work should consider applying QSM to measure Y_v beyond the major draining veins.

5 CONCLUSION

This study compares QSM and TRUST measures of venous oxygenation (Y_v) in patients with sickle cell anemia. QSM and TRUST-based Y_v in the superior sagittal sinus were significantly correlated in healthy controls using all but one TRUST calibration model (HbS_{Bush}). However, in patients with sickle cell anemia, we observed disagreement between QSM and TRUST measures of venous oxygen saturation in the superior sagittal sinus. QSM measures of Y_v suggested decreased Y_v in SCA relative to healthy controls in agreement with TRUST measures of Y_v using a bovine hemoglobin calibration model and previous studies using asymmetric spin-echo methods. This is opposite to the increased Y_v in SCA relative to healthy controls found here and in previous studies using TRUST methods based on sickle hemoglobin calibration models. Further validation of all MRI measures of Y_v, relative to ground truth measures such as O^{15} PET and jugular vein catheterization, is required in SCA before QSM or TRUST methods can be considered for neurological risk prediction in clinical practice.

DATA AVAILABILITY STATEMENT

Full anonymized data will be shared on request from qualified investigators.

ETHICS STATEMENT

The studies involving human participants were reviewed and approved by the West London NHS (05/Q0408/42, 11/EM/0084, 15/LO/0347) Yorkshire NHS (15/YH/0213) University College London (14475/001). Written informed consent to participate in this study was provided by the participants' legal guardian/next of kin.

AUTHOR CONTRIBUTIONS

RM: manuscript preparation, QSM data processing. HS: manuscript preparation, data acquisition, TRUST data processing. PH: TRUST data processing. JK: data acquisition. MK: data acquisition. CC: manuscript review, oversaw set-up of imaging protocol. FK: manuscript review, data acquisition. KS: manuscript review, QSM data processing.

FUNDING

HS and MK were funded by Action Medical Research (GN2509) and JK by Great Ormond Street Children's Charity (V4615). The work was supported by the National Institute for Health Research Biomedical Research Centre (IS-BRC-1215–20012) at Great Ormond Street Hospital for Children NHS Foundation Trust and University College London. The work was supported by a UCL Grand Challenges Doctoral Students Grant. KS is funded by European Research Council Consolidator Grant DiSCo MRI SFN 770939. RM was supported by the EPSRC-funded UCL Centre for Doctoral Training in Medical Imaging (EP/L016478/1) and the Department of Health's NIHR-funded Biomedical Research Centre at Great Ormond Street Hospital (IS-BRC-1215–20012).

ACKNOWLEDGMENTS

The authors would like to thank the patients and controls who participated in this research and their families. They would also like to thank the Great Ormond Street Hospital research radiographers for their efforts: Tina Banks, Jessica Cooper, Nichola Sellers, Paul Xavier, Bella Said, Jorvaar Gill, and Michelle Quigley.

SUPPLEMENTARY MATERIAL

The Supplementary Material for this article can be found online at: https://www.frontiersin.org/articles/10.3389/fphys.2022.913443/full#supplementary-material

REFERENCES

Adams, R. J. (1995). Sickle Cell Disease and Stroke. *J. Child. Neurol.* 10 (2), 75–76. doi:10.1177/088307389501000201

Berg, R. C., Preibisch, C., Thomas, D. L., Shmueli, K., and Biondetti, E. (2021). Investigating the Effect of Flow Compensation and Quantitative Susceptibility Mapping Method on the Accuracy of Venous Susceptibility Measurement. *NeuroImage* 240, 118399. doi:10.1016/j.neuroimage.2021.118399

Biondetti, E., Rojas-Villabona, A., Sokolska, M., Pizzini, F. B., Jäger, H. R., Thomas, D. L., et al. (2019). Investigating the Oxygenation of Brain Arteriovenous Malformations Using Quantitative Susceptibility Mapping. *Neuroimage* 199, 440–453. doi:10.1016/j.neuroimage.2019.05.014

Bush, A., Borzage, M., Detterich, J., Kato, R. M., Meiselman, H. J., Coates, T., et al. (2017). Empirical Model of Human Blood Transverse Relaxation at 3 T Improves MRI T2oximetry. *Magn. Reson. Med.* 77 (6), 2364–2371. doi:10.1002/mrm.26311

Bush, A. M., Borzage, M. T., Choi, S., Václavů, L., Tamrazi, B., Nederveen, A. J., et al. (2016). Determinants of Resting Cerebral Blood Flow in Sickle Cell Disease. *Am. J. Hematol.* 91 (9), 912–917. doi:10.1002/ajh.24441

Bush, A. M., Coates, T. D., and Wood, J. C. (2018). Diminished Cerebral Oxygen Extraction and Metabolic Rate in Sickle Cell Disease Using T2 Relaxation under Spin Tagging MRI. *Magn. Reson. Med.* 80 (1), 294–303. doi:10.1002/mrm.27015

Bush, A., Vu, C., Choi, S., Borzage, M., Miao, X., Li, W., et al. (2021). Calibration of T 2 Oximetry MRI for Subjects with Sickle Cell Disease. *Magn. Reson Med.* 86 (2), 1019–1028. doi:10.1002/mrm.28757

Castro, O. L., Haddy, T. B., and Rana, S. R. (1987). Age- and Sex-Related Blood Cell Values in Healthy Black Americans. *Public Health Rep.* 102 (2), 232–237.

Connes, P., Alexy, T., Detterich, J., Romana, M., Hardy-Dessources, M.-D., Ballas, S. K., et al. (2016). The Role of Blood Rheology in Sickle Cell Disease. *Blood Rev.* 30 (2), 111–118. doi:10.1016/j.blre.2015.08.005

Debaun, M. R., and Kirkham, F. J. (2016). Central Nervous System Complications and Management in Sickle Cell Disease. *Blood* 127 (7), 829–838. doi:10.1182/blood-2015-09-618579

Eldeniz, C., Binkley, M. M., Fields, M., Guilliams, K., Ragan, D. K., Chen, Y., et al. (2021). Bulk Volume Susceptibility Difference between Deoxyhemoglobin and Oxyhemoglobin for HbA and HbS: A Comparative Study. *Magn. Reson Med.* 85 (6), 3383–3393. doi:10.1002/mrm.28668

Fan, A. P., KhalilKhalil, A. A., Fiebach, J. B., Zaharchuk, G., Fiebach, J. B., Zaharchuk, G., et al. (2020). Elevated Brain Oxygen Extraction Fraction Measured by MRI Susceptibility Relates to Perfusion Status in Acute Ischemic Stroke. *J. Cereb. Blood Flow Metab.* 40 (3), 539–551. doi:10.1177/0271678x19827944

Fields, M. E., Guilliams, K. P., Ragan, D. K., Binkley, M. M., Eldeniz, C., Chen, Y., et al. (2018). Regional Oxygen Extraction Predicts Border Zone Vulnerability to Stroke in Sickle Cell Disease. *Neurology* 90 (13), e1134–e1142. doi:10.1212/wnl.0000000000005194

Hales, P. W., Kirkham, F. J., and Clark, C. A. (2016). A General Model to Calculate the Spin-Lattice (T1) Relaxation Time of Blood, Accounting for Haematocrit, Oxygen Saturation and Magnetic Field Strength. *J. Cereb. Blood Flow. Metab.* 36 (2), 370–374. doi:10.1177/0271678x15605856

Herity, L. B., Vaughan, D. M., Rodriguez, L. R., and Lowe, D. K. (2021). Dale Marie M. Vaughan, Lindsey Ritenour Rodriguez, and Denise Kozella LoweVoxelotor: A Novel Treatment for Sickle Cell Disease. *Ann. Pharmacother.* 55 (2), 240–245. doi:10.1177/1060028020943059

Herold, S., Brozovic, M., Gibbs, J., Lammertsma, A. A., Leenders, K. L., Carr, D., et al. (1986). Measurement of Regional Cerebral Blood Flow, Blood Volume and Oxygen Metabolism in Patients with Sickle Cell Disease Using Positron Emission Tomography. *Stroke* 17 (4), 692–698. doi:10.1161/01.str.17.4.692

Howard, J., April, E. S., Skene, S., Inusa, B., Kawadler, J., Downes, M., et al. (2018). Overnight Auto-Adjusting Continuous Airway Pressure+standard Care Compared with Standard Care Alone in the Prevention of Morbidity in Sickle Cell Disease Phase II (POMS2b): Study Protocol for a Randomised Controlled Trial. *Trials* 19 (1), 1–10. doi:10.1186/s13063-017-2419-0

Jain, V., Abdulmalik, O., Propert, K. J., and Wehrli, F. W. (2012). Investigating the Magnetic Susceptibility Properties of Fresh Human Blood for Noninvasive Oxygen Saturation Quantification. *Magn. Reson. Med.* 68 (3), 863–867. doi:10.1002/mrm.23282

Jordan, L. C., Gindville, M. C., Scott, A. O., Juttukonda, M. R., Strother, M. K., Kassim, A. A., et al. (2016). "Non-Invasive Imaging of Oxygen Extraction Fraction in Adults with Sickle Cell Anaemia." *Brain* 139 (3), 738–750. doi:10.1093/brain/awv397

Jordan, L. C., and DeBaun, M. R. (2018). Cerebral Hemodynamic Assessment and Neuroimaging across the Lifespan in Sickle Cell Disease. *J. Cereb. Blood Flow. Metab.* 38 (9), 1438–1448. doi:10.1177/0271678x17701763

Karsa, A., and Shmueli, K. (2018). SEGUE: A Speedy Region-Growing Algorithm for Unwrapping Estimated Phase. *IEEE Trans. Med. Imaging* 38 (6), 1347–1357. doi:10.1109/TMI.2018.2884093

Karsa, A., Punwani, S., and Shmueli, K. (2020). An Optimized and Highly Repeatable MRI Acquisition and Processing Pipeline for Quantitative Susceptibility Mapping in the Head-And-Neck Region. *Magn. Reson Med.* 84, 3206–3222. doi:10.1002/mrm.28377

Kiersnowski, Oliver C., Karsa, A., Wastling, S. J., Thornton, J. S., and Shmueli, K. (2021). The Effect of Oblique Image Acquisition on the Accuracy of Quantitative Susceptibility Mapping and a Robust Tilt Correction Method. *bioRxiv*.

Kratz, A., Ferraro, M., Sluss, P. M., and Lewandrowski, K. B. (2004). Laboratory Reference Values. *New England J. Med.* 351, 1548–1564.

Kudo, K., Liu, T., Murakami, T., Goodwin, J., Uwano, I., Yamashita, F., et al. (2016). Oxygen Extraction Fraction Measurement Using Quantitative Susceptibility Mapping: Comparison with Positron Emission Tomography. *J. Cereb. Blood Flow. Metab.* 36 (8), 1424–1433. doi:10.1177/0271678x15606713

Li, W., Xu, X., Liu, P., Strouse, J. J., Casella, J. F., Lu, H., et al. (2020). Quantification of Whole-Brain Oxygenation Extraction Fraction and Cerebral Metabolic Rate of Oxygen Consumption in Adults with Sickle Cell Anemia Using Individual T_2 -based Oxygenation Calibrations. *Magn. Reson Med.* 83 (3), 1066–1080. doi:10.1002/mrm.27972

Lin, Z., McIntyre, T., Jiang, D., Cannon, A., Liu, P., Tekes, A., et al. (2022). Brain Oxygen Extraction and Metabolism in Pediatric Patients with Sickle Cell Disease: Comparison of Four Calibration Models. *Front. Physiology* 13 (February), 1–11. doi:10.3389/fphys.2022.814979

Liu, T., Khalidov, I., de Rochefort, L., Spincemaille, P., Liu, J., Tsiouris, A. J., et al. (2011). A Novel Background Field Removal Method for MRI Using Projection onto Dipole Fields (PDF). *NMR Biomed.* 24 (9), 1129–1136. doi:10.1002/nbm.1670

Liu, T., Wisnieff, C., Lou, M., Chen, W., Spincemaille, P., and Wang, Y. (2013). Nonlinear Formulation of the Magnetic Field to Source Relationship for Robust Quantitative Susceptibility Mapping. *Magn. Reson Med.* 69 (2), 467–476. doi:10.1002/mrm.24272

Lu, H., Xu, F., Grgac, K., Liu, P., Qin, Q., and Van Zijl, P. (2012). Calibration and Validation of TRUST MRI for the Estimation of Cerebral Blood Oxygenation. *Magn. Reson. Med.* 67 (1), 42–49. doi:10.1002/mrm.22970

McFadden, J. J., Matthews, J. C., Lauren, A. S., Parker, G. J. M., Lohézic, M., and Parkes, L. M. (2021). Optimization of Quantitative Susceptibility Mapping for Regional Estimation of Oxygen Extraction Fraction in the Brain. *Magnetic Reson. Med.*, 86(3) 1–16. doi:10.1002/mrm.28789

Modat, M., Cash, D. M., Daga, P., Winston, G. P., Duncan, J. S., and Ourselin, S. (2014). Global Image Registration Using a Symmetric Block-Matching Approach. *J. Med. Imag.* 1 (2), 024003. doi:10.1117/1.jmi.1.2.024003

Murdoch, R., Kawadler, J., Carmichael, D., Kirkham, F., and Shmueli, K. (2020). "Can Multi-Parametric Mapping Sequences Be Used for Accurate Quantitative Susceptibility Mapping?," in Proceedings of the 2020 ISMRM and SMRT Virtual Conference and Exhibition. (International Society for Magnetic Resonance in Medicine (ISMRM)).

Murdoch, R., Stotesbury, H., Kawadler, J., Saunders, D., Kirkham, F., and Shmueli, K. (2021). "Investigating the Effect of Positive Airways Pressure on Venous Oxygenation in Sickle Cell Anemia with Quantitative Susceptibility Mapping," in Proceedings of the 2021 ISMRM and SMRT Annual Meeting and Exhibition. (International Society for Magnetic Resonance in Medicine (ISMRM)).

Pavlakis, S. G., and Levinson, K. (2009). Arterial Ischemic Stroke: Common Risk Factors in Newborns and Children. *Stroke* 40 (3 Suppl.), S79–S81. doi:10.1161/STROKEAHA.108.531749

Rosen, C. L., Debaun, M. R., Strunk, R. C., Redline, S., Seicean, S., Craven, D. I., et al. (2014). Obstructive Sleep Apnea and Sickle Cell Anemia. *Pediatrics* 134 (2), 273–281. doi:10.1542/peds.2013-4223

Shen, J., Coates, T., and Wood, J. C. (2019). Lower Oxygen Saturation in the Internal Cerebral Vein of Patients with Sickle Cell Disease Revealed by Qsm-MRI. *Blood* 134, 984. doi:10.1182/blood-2019-131968

Shmueli, K. (2020). "Quantitative Susceptibility Mapping," in *Quantitative Magnetic Resonance Imaging* (Academic Press), Cambridge, Massachusetts, United States, 1, 819–838. doi:10.1016/b978-0-12-817057-1.00033-0

Smith, S. M. (2002). Fast Robust Automated Brain Extraction. *Hum. Brain Mapp.* 17 (3), 143–155. doi:10.1002/hbm.10062

Stotesbury, H., Kawadler, J. M., Hales, P. W., Saunders, D. E., Clark, C. A., and Kirkham, F. J. (2019). Vascular Instability and Neurological Morbidity in Sickle Cell Disease: An Integrative Framework. *Front. Neurol.* 10 (AUG), 21. doi:10.3389/fneur.2019.00871

Stotesbury, H., Hales, P. W., Koelbel, M., Hood, A. M., Kawadler, J. M., Saunders, D. E., et al. (2022). Venous Cerebral Blood Flow Quantification and Cognition in Patients with Sickle Cell Anemia. *J. Cereb. Blood Flow. Metabolism.* 42(6): 1061–1077. doi:10.1177/0271678x211072391

Stotesbury, H., Hales, P. W., and Kirkham, F. J. (2018). The Promise of Noninvasive Cerebral Hemodynamic Assessment in Sickle Cell Anemia. *Neurology* 90 (13), 585–586. doi:10.1212/wnl.0000000000005236

Stotesbury, H., Kawadler, J. M., Saunders, D. E., and Kirkham, F. J. (2021). MRI Detection of Brain Abnormality in Sickle Cell Disease. *Expert Rev. Hematol.* 14 (5), 473–491. doi:10.1080/17474086.2021.1893687

Vu, C., Bush, A., Choi, S., Borzage, M., Miao, X., Nederveen, A. J., et al. (2021). Reduced Global Cerebral Oxygen Metabolic Rate in Sickle Cell Disease and Chronic Anemias. *Am. J Hematol* 96 (8), 901–913. doi:10.1002/ajh.26203

Weiskopf, N., Suckling, J., Williams, G., Correia, M. M., Inkster, B., Tait, R., et al. (2013). Quantitative Multi-Parameter Mapping of R1, PD(*), MT, and R2(*) at 3T: A Multi-Center Validation. *Front. Neurosci.* 7 (7 JUN), 95. doi:10.3389/fnins.2013.00095

Weisskoff, R. M., and Kiihne, S. (1992). MRI Susceptometry: Image-Based Measurement of Absolute Susceptibility of MR Contrast Agents and Human Blood. *Magn. Reson Med.* 24 (24), 375–383. doi:10.1002/mrm.1910240219

Yushkevich, P. A., Piven, J., Hazlett, H. C., Smith, R. G., Ho, S., Gee, J. C., et al. (2006). User-Guided 3D Active Contour Segmentation of Anatomical Structures: Significantly Improved Efficiency and Reliability. *NeuroImage* 31 (3), 1116–1128. doi:10.1016/j.neuroimage.2006.01.015

Zaitsu, Y., Kudo, K., Terae, S., Yazu, R., Ishizaka, K., Fujima, N., et al. (2011). Mapping of Cerebral Oxygen Extraction Fraction Changes with Susceptibility-Weighted Phase Imaging. *Radiology* 261 (3), 930–936. doi:10.1148/radiol.11102416

Conflict of Interest: The authors declare that the research was conducted in the absence of any commercial or financial relationships that could be construed as a potential conflict of interest.

Publisher's Note: All claims expressed in this article are solely those of the authors and do not necessarily represent those of their affiliated organizations, or those of the publisher, the editors and the reviewers. Any product that may be evaluated in this article, or claim that may be made by its manufacturer, is not guaranteed or endorsed by the publisher.